

Is a box model effective for understanding the carbon cycle?

Akira Tomizuka

Citation: *American Journal of Physics* **77**, 156 (2009); doi: 10.1119/1.3013196

View online: <http://dx.doi.org/10.1119/1.3013196>

View Table of Contents: <http://aapt.scitation.org/toc/ajp/77/2>

Published by the *American Association of Physics Teachers*



American Association of **Physics Teachers**

Explore the **AAPT Career Center** –
access hundreds of physics education and
other STEM teaching jobs at two-year and
four-year colleges and universities.

<http://jobs.aapt.org>



Is a box model effective for understanding the carbon cycle?

Akira Tomizuka^{a)}

Faculty of Environmental Studies, Nagasaki University, 1-14 Bunkyo-machi, Nagasaki 852-8521, Japan

(Received 19 November 2007; accepted 14 October 2008)

A seven-box carbon cycle model is used to show the time dependence of atmospheric CO₂ for the past 250 years and the current flux between individual reservoirs. The model also yields results for future levels of atmospheric CO₂ based on various scenarios. © 2009 American Association of Physics Teachers.

[DOI: 10.1119/1.3013196]

I. INTRODUCTION

To what extent do we really understand the environmental issues we face? Many citizens as well as researchers simply accept the opinion of experts. One reason is that the Earth system is complex and environmental issues are associated with diverse natural phenomena. Specialists calculate atmospheric flow using complex models and predict climate change and its influence on Earth. For such work they have little choice but to use black box systems such as the “Earth Simulator.”¹

The climate of Earth has changed in the past without human interference. However, for the past 11 000 years, Earth has been mostly in a state of equilibrium. Humans have disturbed this equilibrium by the rapid release of CO₂ to the atmosphere. The response of the global system to this perturbation manifests itself as climate change.

The interactions of the atmosphere, geosphere, and hydrosphere are complex, only some of which are well understood. The associated equations involve too many variables to allow a simple picture of the system. The simplification provided by box models allow judgments of what to simplify.² The boxes represent large reservoirs of a material. Box models are widely utilized for the flow of pollutants and the global circulation of various materials.²

In this paper we discuss the validity of box models to reproduce the trend of CO₂ concentration in the atmosphere, for determining the flux among carbon reservoirs, and for projecting future CO₂ concentrations. Although these models need not be perfect to promote understanding, they must achieve a reasonable level of accuracy to be useful.

II. INVESTIGATION USING THE SIMPLE TWO-BOX MODEL

Carbon cycle models include box models, box diffusion models (models that include vertical diffusion of the carbon in the ocean to the box models),³ and advective-diffusion models (models that add convection of the carbon in the ocean to the box diffusion models).⁴ Box models are the most intuitive and easy to understand. A box represents a well-mixed reservoir, and the flux from a box is proportional to its content in the reservoir. As a first approximation, carbon flux in the environment can be thought of as flux between two reservoirs, the atmosphere and the surface of the ocean. This approximation means that the net CO₂ flux between the atmosphere and the terrestrial biosphere is balanced for the period of interest, and the uptake of CO₂ by the intermediate and deep levels of the ocean is small.

Figure 1 shows a simple two-box model, which is modified from the multiple carbon cycle model.⁵ The content of

740 PgC (1 PgC = 10¹⁵ g of carbon) in the atmosphere corresponds to 347 ppm (parts per million) in 1986. The value of CO₂ concentration in ppm is found by dividing the carbon content in PgC by 2.13.

A simple rate equation models the flow between these reservoirs:

$$\frac{dN_1}{dt} = -k_{12}N_1 + k_{21}N_2 + \gamma, \quad (1)$$

$$\frac{dN_2}{dt} = k_{12}N_1 - k_{21}N_2, \quad (2)$$

where N_1 and N_2 denote the concentration of carbon in the atmosphere and the surface of the ocean, respectively, t is the time, and the transfer coefficient k_{ij} is the ratio of carbon flux from reservoir i to j divided by the carbon content in reservoir i : $k_{12} = 105/740$ and $k_{21} = 102/900$. These numbers are shown in Fig. 1.

The CO₂ uptake by the ocean is suppressed by the large amount of dissolved inorganic carbon in the ocean. This effect is expressed by the buffer factor ξ . It depends on the CO₂ concentration in the atmosphere and is approximated as a quadratic function of the concentration (see the Appendix). In the preindustrial era the equilibrium value of carbon in the surface ocean was N_2^0 , and the flux from the surface ocean to the atmosphere was $k_{21}N_2^0$. The extra flux that originates in the increase from equilibrium is $k_{21}\xi(N_2 - N_2^0)$. Equations (1) and (2) are modified by the buffer effect as

$$\frac{dN_1}{dt} = -k_{12}N_1 + k_{21}(N_2^0 + \xi(N_2 - N_2^0)) + \gamma, \quad (3)$$

$$\frac{dN_2}{dt} = k_{12}N_1 - k_{21}(N_2^0 + \xi(N_2 - N_2^0)), \quad (4)$$

where γ is the rate of production of CO₂ by fossil-fuel burning. This rate is available for the years 1750 to 2003 at the Carbon Dioxide Information Analysis Center (CDIAC) website, which provides data related to greenhouse gases and their influence.⁶

Equations (3) and (4) require the equilibrium value N_2^0 . Keeling *et al.* have pointed out that the observed fraction of industrial emission in the atmosphere from 1959 to 1979 remained approximately constant at 56%.⁷ If the remainder is assumed to be taken up by the ocean, the 79 PgC that corresponds to 44% of the total industrial emission up to 1986 may be added to the surface ocean. Therefore, we let $N_2^0 = 900 - 79 = 821$. Because the data for anthropogenic CO₂ and atmospheric CO₂ concentrations are available annually, the

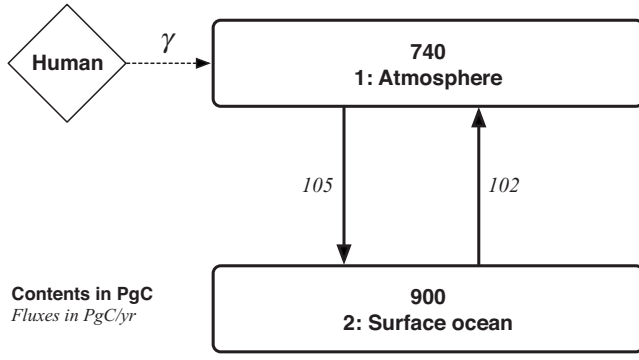


Fig. 1. The simple two-box model for the global carbon cycle, which is modified from the multiple carbon cycle model. (Ref. 5). The content of 740 PgC in the atmosphere corresponds to 347 ppm in 1986.

time t is expressed in years. Equations (3) and (4) are solved numerically as difference equations with $\Delta t=1$ and given initial values. The results with a smaller value of Δt were unchanged.

Figure 2 shows the calculated CO_2 concentration in the atmosphere from 1987 to 2003 (solid line). It also shows the observed values at Mauna Loa (dots) and the result without the buffer effect ($\xi=1$) (fine line). The Mauna Loa data set is a precise record and a reliable indicator of the atmospheric CO_2 concentration in the middle layers of the troposphere.⁸ We see the big difference after 1987 resulting from the “sudden” buffer effect. This difference can be understood by beginning the calculation with the equilibrium values in the preindustrial era. The increasing atmospheric CO_2 with the buffer effect is bigger than the one without buffer effect. We see that the model without the buffer effect corresponds more closely to the observed value. This result means that the buffer effect increases the carbon that stays in the atmosphere, and the increased carbon has been absorbed in other carbon sinks. We conclude that the two-box model is insufficient to describe the carbon cycle and improvements are needed.

A more appropriate model needs to reproduce the trend of CO_2 over the past 250 years since industrialization. To do so, three other ocean reservoirs (the intermediate ocean, the deep ocean, and the sediments), and emission by land-use change, for example by deforestation, must be considered. Because

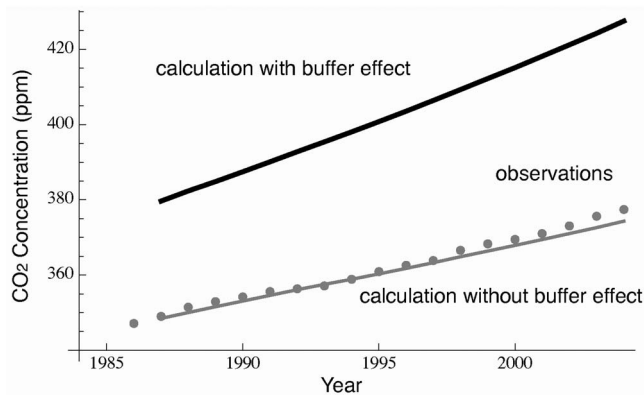


Fig. 2. The CO_2 trend predicted by the two-box model with the buffer effect (solid line). The observed values and the result without the buffer effect are shown by dots and a fine line, respectively.

the total emission by land-use change for the past 250 years is about 190 PgC,⁹ which is almost two-thirds of that from fossil-fuel burning, its emission cannot be disregarded. It also is necessary to consider at least two reservoirs (the terrestrial biosphere and the soil) when land-use change is included.

III. VERIFICATION OF THE TREND PREDICTED BY THE SEVEN-BOX MODEL

It is necessary to include CO_2 uptake by the terrestrial biosphere and CO_2 emission by land-use change in the model. The most commonly used form for CO_2 flux to the biosphere is logarithmic and is expressed as¹⁰

$$f = f^0(1 + \beta \ln(P/P^0)), \quad (5)$$

where f is the net primary productivity (the difference between the carbon uptake rate by photosynthesis and the carbon emission rate by respiration); f^0 corresponds to the preindustrial value of f . P is the atmospheric CO_2 concentration, and P^0 is the preindustrial value of P . The fertilization factor, or β factor, is often chosen to be around 0.42.¹¹ This factor will be treated as a parameter because its value changes with atmospheric temperature, soil water, and plant type.¹²

CO_2 emission to the atmosphere by changes in land-use was estimated by Houghton *et al.* and data from 1850 to 2000 are available.⁹ The trend before 1850 is obtained by linearly interpolating from 0.2 PgC/year in 1750 to 0.5 PgC/year in 1850.¹³

The emission of CO_2 to the atmosphere by changes in land use, and the carbon circulation in the terrestrial ecosystem are given as follows. Half of the carbon released from trees is transferred to the atmosphere by burning or rapid decomposition. The other half is transferred to the soil. Twice the amount of carbon transferred to the atmosphere will be lost from trees.¹⁴

A representation of the seven-box model including the atmosphere, the terrestrial biosphere, the soil, the surface ocean, the intermediate ocean, the deep ocean, and sediments is presented in Fig. 3.¹⁵ The rate equation for each reservoir is given as

$$\begin{aligned} \frac{dN_1}{dt} = & -k_{12}N_1 + k_{21}(N_2^0 + \xi(N_2 - N_2^0)) + \gamma - f + \delta + k_{51}N_5 \\ & + k_{71}N_7, \end{aligned} \quad (6)$$

$$\begin{aligned} \frac{dN_2}{dt} = & k_{12}N_1 - k_{21}(N_2^0 + \xi(N_2 - N_2^0)) - k_{23}N_2 + k_{32}N_3 \\ & - k_{24}N_2, \end{aligned} \quad (7)$$

$$\frac{dN_3}{dt} = k_{23}N_2 - k_{32}N_3 - k_{34}N_3 + k_{43}N_4, \quad (8)$$

$$\frac{dN_4}{dt} = k_{34}N_3 - k_{43}N_4 + k_{24}N_2 - k_{45}N_4, \quad (9)$$

$$\frac{dN_5}{dt} = k_{45}N_4 - k_{51}N_5, \quad (10)$$

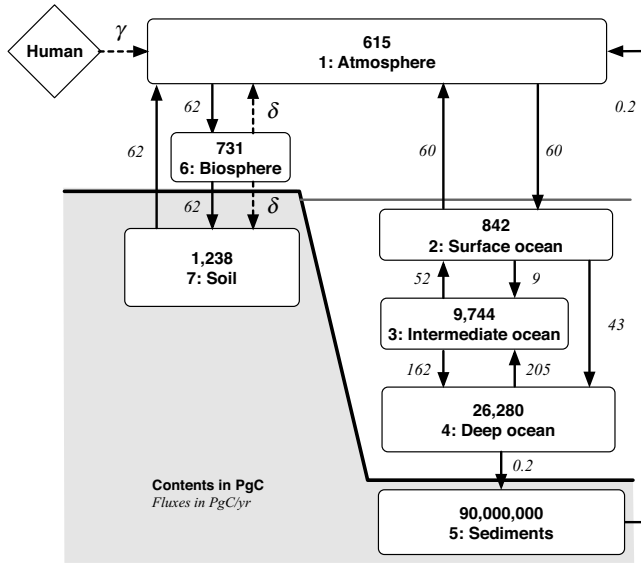


Fig. 3. The seven-box model for the global carbon cycle. The assumed values of the content and flux in the preindustrial era are expressed in PgC and PgC/yr, respectively (mainly based on Fig. 11.8 in Ref. 15).

$$\frac{dN_6}{dt} = f - k_{67}N_6 - 2\delta, \quad (11)$$

$$\frac{dN_7}{dt} = k_{67}N_6 - k_{71}N_7 + \delta. \quad (12)$$

N_i denotes the time-dependent content of carbon in reservoir i , and k_{ij} is the transfer coefficient of the carbon flux from reservoir i to reservoir j . The subscript 1 refers to the atmosphere, 2 to the surface ocean, 3 to the intermediate ocean, 4 to the deep ocean, 5 to the sediments, 6 to the terrestrial biosphere, and 7 to the soil. N_2^0 is the equilibrium value of N_2 in the preindustrial era, γ is the emission rate to the atmosphere by the burning of fossil fuel, and δ is the emission rate to the atmosphere by changes in land use.

The assumed values of the content and flux in 1750 when the simulation begins are shown in Fig. 3. We take $f^0 = 62$ PgC/year. The transfer coefficients are

$$\begin{aligned} k_{12} &= 60/615, \\ k_{21} &= 60/842, \quad k_{23} = 9/842, \quad k_{24} = 43/842, \\ k_{32} &= 52/9744, \quad k_{34} = 162/9744, \\ k_{43} &= 205/26280, \quad k_{45} = 0.2/26280, \\ k_{51} &= 0.2/90\,000\,000, \\ k_{67} &= 62/731, \\ k_{71} &= 62/1328. \end{aligned} \quad (13)$$

The numerical values of the coefficients are shown in Fig. 3.

The atmospheric CO_2 concentration before the industrial era is equivalent to 289 ppm. Although this value is 10 ppm higher than the ice core data, it has been used in many simulations.^{10,14} Equations (5)–(12) are solved iteratively for 250 years.

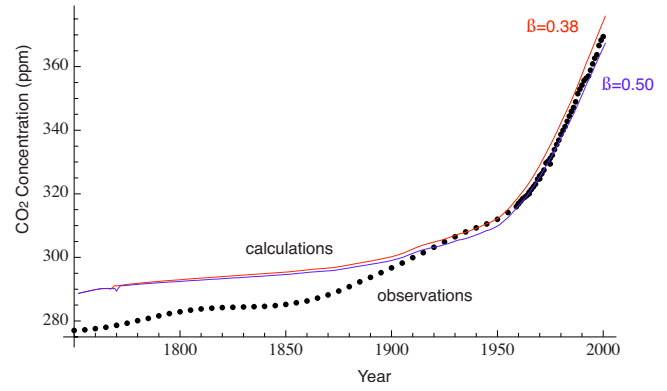


Fig. 4. The CO_2 trend calculated for 250 years by the seven-box model with $\beta=0.38$ and 0.50. The observed values are shown for reference.

Figure 4 shows the calculated values of atmospheric CO_2 with $\beta=0.38$ and 0.50. The assumed values from the ice cores from Antarctica until 1960 and the observed values at Mauna Loa after 1960 are shown for comparison.¹⁶ Although there is a difference of 10 ppm in the initial value, the behavior of $N_i(t)$ is reasonable and reproducibility after 1960 is especially good. Figure 4 also shows that the fertilization factor β does not have too big an influence on the result.

Next we compare the mean simulated values of the fluxes among the reservoirs in the 1980s and the 1990s with the values given in the Intergovernmental Panel on Climate Change (IPCC) Third Assessment Report based on more precise models.¹⁷ Some of these data are compared with the values in the Fourth Assessment Report.¹⁸

Table I shows comparison of the IPCC values and our calculated values, with the parameter β is chosen to have the possible values of 0.38, 0.42, 0.46, and 0.50. The fluxes were obtained by the following calculations:

Atmospheric increase:

$$dN_1/dt, \quad (14)$$

Ocean-atmosphere flux:

$$-k_{12}N_1 + k_{21}(N_2^0 + \xi(N_2 - N_2^0)), \quad (15)$$

Land-atmosphere flux:

$$k_{71}N_7 - f^0(1 + \beta \ln(P_1/P_1^0)) + \delta, \quad (16)$$

Residual terrestrial sink:

$$k_{71}N_7 - f^0(1 + \beta \ln(P_1/P_1^0)). \quad (17)$$

The values of the simulated atmosphere from the seven-box model and evaluated values in the IPCC reports correspond closely in terms of the atmospheric increase and the ocean-atmosphere flux observed during these two decades from Table I. However, there is a clear difference in the values that relate to land-use change. One of the causes is that the land-atmosphere flux is estimated in the Third Assessment Report,¹⁷ as the result of removing the atmospheric increase and the ocean-atmosphere flux from fossil-fuel emission. In addition, the residual terrestrial sink is estimated by removing the land-use change flux from the land-atmosphere flux. In contrast, the residual terrestrial sink in the simulation is obtained directly from the flux from the soil and the uptake

Table I. Comparison of the calculated global CO₂ fluxes and the atmospheric concentration with the Third Assessment Report estimates for the 1980s and 1990s, fluxes are expressed in PgC/yr, and the concentration in ppm.

	Third assessment report	β			
		0.38	0.42	0.46	0.50
1980s					
Emissions	5.4 ± 0.3	5.5	5.5	5.5	5.5
Atmospheric increase	3.3 ± 0.1	3.2	3.1	3.0	2.9
Ocean-atmosphere flux	-1.9 ± 0.6	-1.3	-1.3	-1.3	-1.2
Land-atmosphere flux	-0.2 ± 0.7	-1.1	-1.3	-1.4	-1.6
Land-use change flux	$1.7(0.6 \text{ to } 2.5)^a$	2.0	2.0	2.0	2.0
Residual terrestrial sink	$-1.9 (-3.8 \text{ to } 0.3)^b$	-3.1	-3.3	-3.4	-3.6
Atmospheric concentration	352.9	355.8	353.6	351.6	349.6
1990s					
Emissions	6.4 ± 0.4	6.5	6.5	6.5	6.5
Atmospheric increase	3.2 ± 0.1	3.6	3.4	3.3	3.2
Ocean-atmosphere flux	-1.7 ± 0.5	-1.6	-1.5	-1.5	-1.5
Land-atmosphere flux	-1.4 ± 0.7	-1.5	-1.7	-1.9	-2.1
Land-use change flux	NA ^c	2.2	2.2	2.2	2.2
Residual terrestrial sink	NA ^d	-3.7	-3.9	-4.1	-4.2
Atmospheric concentration	368.3	372.6	369.8	367.1	364.5

^aAR4 (IPCC Fourth Assessment Report) revised the value as 1.4 (0.4 to 2.3) (Ref. 18).

^bAR4 revised the value as -1.7 (-3.4 to 0.2).

^cAR4 estimates this as 1.6 (0.5 to 2.7).

^dAR4 estimates this as -2.6 (-4.3 to -0.9).

flux by the biosphere, and becomes the land-atmosphere flux by adding the deforestation flux as shown in Eq. (16). Another reason is that there is much uncertainty about the trend of carbon uptake in the terrestrial biosphere. The land-use change data in the Third Assessment Report¹⁷ or the Fourth Assessment Report¹⁸ listed in Table I show the ranges based on the CDAIC and other datasets.

We conclude that the results of the seven-box as shown in Fig. 4 are acceptable. The control parameter β is chosen to be 0.42, a typical value. Its precise value is not important because the results do not depend sensitively on its value.

IV. FUTURE FORECASTS OF THE SEVEN-BOX MODEL

In this section we compare the projections of the seven-box model with the projections in the Third Assessment Report.¹⁷ These projections are the atmospheric CO₂ concentration over a 100-year interval based on the scenarios of the Special Report on Emissions Scenarios (SRES), and the emission rate of the anthropogenic CO₂ necessary to achieve the WRE (Wigley, Richels, and Edmonds) stabilization profiles.¹⁹

A. Projected CO₂ concentration based on SRES scenarios

The SRES long-term emissions scenarios summarize the future emissions forecast (1990 to 2100) of greenhouse gases including CO₂ according to the driving forces of demographic change, socio-economic development, and technological change.²⁰ The scenario consists of six groups: (1) dependent on fossil energy sources, (2) dependent on non-fossil energy sources, (3) emphasis on the balance among various energy sources, (4) multipolarized society, (5) sus-

tainable growth oriented society, and (6) emphasis on regional initiatives. Figure 5 shows global annual CO₂ emission by (a) fossil-fuel burning and by (b) land-use change based on the six scenarios.

In the following the projected atmospheric CO₂ concentrations for a 100-year period calculated using the seven-box model are compared with the results by the ISAM (Integrated Science Assessment Model)²¹ in the Third Assessment Report.¹⁷ The ISAM is mainly comprised of a vertical diffusion ocean model, a six-box terrestrial model, and the radiative forcing modules. The projected values in the ISAM model are calculated with varying climate sensitivities from 1.5 to 4.5 °C for a doubling of CO₂. Climate sensitivity refers to the volatility of the global temperature associated with the change of energy flux that originates in an increase of greenhouse gases. Our simple seven-box model does not include such feedback effects. The high-CO₂ case in the Third Assessment Report is defined by a climate sensitivity of 4.5 °C and minimal CO₂ uptake by the oceans and land; the low-CO₂ case has a climate sensitivity of 1.5 °C and maximal CO₂ uptake by the oceans and land. A reference case is one with climate sensitivity of 2.5 °C and average uptake by oceans and land.

It is preferable that the seven-box model be compared to the low-CO₂ case of the ISAM model because our seven-box model with no feedback can be regarded as having a climate sensitivity of 0 °C and an average CO₂ uptake. The atmospheric CO₂ increase in the low-CO₂ case with 1.5 °C feedback for a doubling of CO₂ must be larger than the seven-box model with 0 °C feedback. CO₂ uptake by the oceans and land in the former is a maximum, and in the latter it is average. The increased CO₂ due to a climate sensitivity of 1.5 °C in comparison with the seven-box model may compensate by a maximum CO₂ uptake by the oceans and land. As a result, the behavior of both models will be similar.

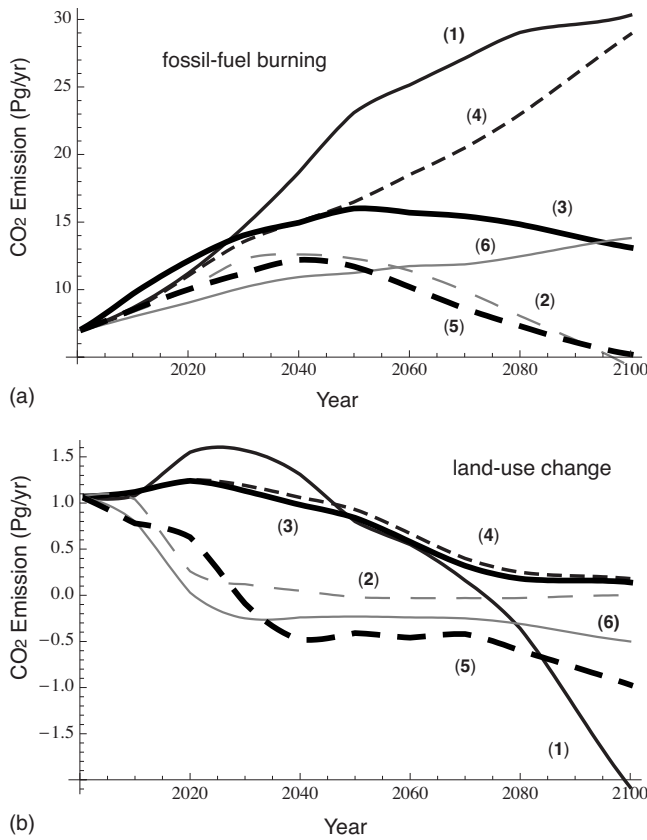


Fig. 5. The CO₂ emissions projected by the six SRES scenarios from (a) fossil-fuel burning and (b) land-use change: (1) dependent on fossil energy sources, (2) dependent on nonfossil energy sources, (3) emphasis on the balance among various energy sources, (4) multipolarized society, (5) sustainable growth oriented society, and (6) emphasis on regional initiatives.

The initial content of each reservoir in the year 2000 was calculated in Sec. III, and the transfer coefficients are also the same. The values of the anthropogenic CO₂ data, γ and δ , are shown in Figs. 5(a) and 5(b), respectively.

Figure 6 shows the projected CO₂ concentrations resulting from the six SRES scenarios using the seven-box model (thick lines), compared with the low-CO₂ case of the ISAM model (thin lines). The seven-box model reproduces the

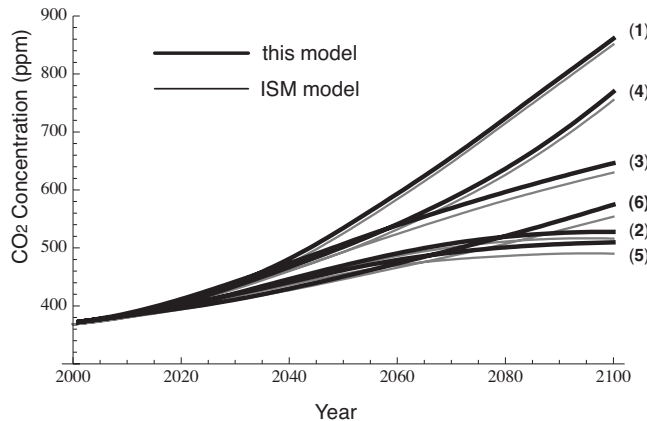


Fig. 6. The projected CO₂ concentrations resulting from the six SRES scenarios using the seven-box model (thick lines). For reference, the low-CO₂ case of the ISAM model is shown with thin lines.

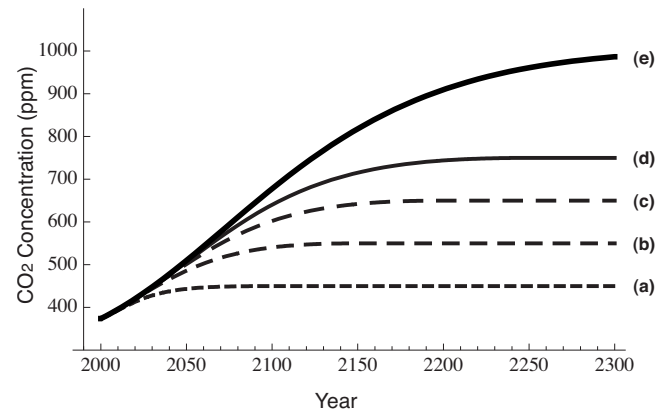


Fig. 7. The WRE profiles stabilized with CO₂ concentrations of (a) 450, (b) 550, (c) 650, (d) 750, and (e) 1000 ppm. The stabilization years are determined as 2100, 2150, 2200, 2250, and 2375, respectively.

features of the ISAM model results very well and is thus an effective representation of the more complex SRES calculations.

B. Stabilization scenarios based on WRE profiles

What reduction plan should we make to stabilize future atmospheric CO₂ concentrations? The WRE profiles were proposed as highly realizable stabilization profiles (see Fig. 7).¹⁹ The trajectories follow realistic CO₂ emissions based on the IS92a scenario in 2030 (Ref. 22) and smoothly reach constant CO₂ concentrations of 450, 550, 650, 750, and 1000 ppm, and do not change afterward.

In this section the CO₂ emission rates produced by fossil-fuel burning needed to achieve the WRE profiles are derived from the seven-box model initialized in the year 2000 and compared with the stabilization scenarios in Third Assessment Report.

The relation between the emission rate of the anthropogenic carbons and the rate of increase of carbon concentration in the atmosphere is shown in Eq. (6). The stabilization emission rate γ is obtained by replacing dN_1/dt by $2.13dW/dt$, where W is the value of the WRE profile shown in Fig. 7 in ppm. We rewrite Eq. (6) as

$$\gamma = 2.13 \frac{dW}{dt} + k_{12}N_1 - k_{21}(N_2^0 + \xi(N_2 - N_2^0)) + f - k_{71}N_7 - k_{51}N_5 - \delta. \quad (18)$$

The initial content in each reservoir in 2000 is as calculated in Sec. III, and the transfer coefficients are the same as in the former. The value of δ in Eq. (18) follows the IS92a scenario from 2000 to 2100 and is assumed to be constant after 2100.

By repeatedly using Eqs. (5), (18), and (7)–(12), the stabilization emission rate may be calculated. Figure 8 shows five projected CO₂ emissions (solid lines) using the seven-box model. The results of the ISAM model which includes feedback effects of climate sensitivity and uptake by oceans and land in the Third Assessment Report are shown as gray areas for comparison. The upper bounds in Fig. 8 are the low CO₂ case of the ISAM model, which are compared with the seven-box model as discussed in Sec. III A. The general features of the seven-box model reproduce the low CO₂ case in the Third Assessment Report well. CO₂ stabilization at 450,

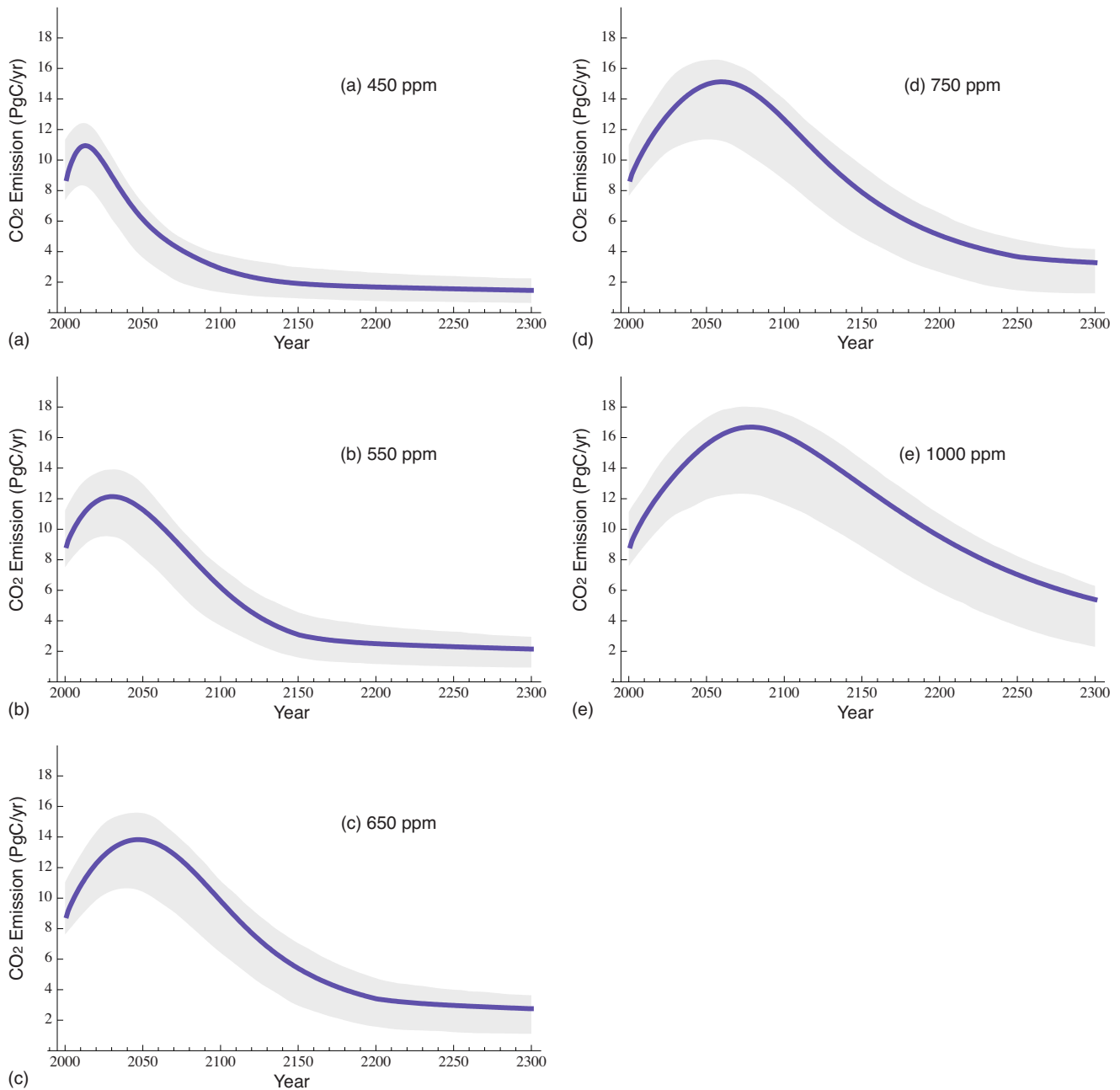


Fig. 8. The projected rates of CO_2 emission based on the WRE stabilization scenarios in Fig. 7. The solid line shows the result of the seven-box model. The gray area is the range enclosed by the upper and lower bounds of the ISAM model, corresponding to the low- and high- CO_2 cases, respectively. The results of the seven-box model without feedback are very similar to the low- CO_2 case in the ISAM model.

550, 650, or 750 ppm would require anthropogenic emission to be suppressed below 1990 levels (6 PgC/year) for a half century, a century, about one and one-half centuries, and about two centuries, respectively, assuming flux from land-use change after 2100 to be -0.1 PgC/year. If there is a delay in achieving CO_2 reduction, the atmospheric CO_2 concentration will become much higher, even if it ultimately stabilizes.

The shape of the stabilization emission is similar to a Gaussian, and the WRE profile looks similar to the error function. As a consequence, the Earth system can be approximately considered to be a linear system for the change of carbon. This linearity can be interpreted as follows.

Equations (5)–(12) and (18) are linear except for the up-

take by the oceans and the biosphere. In addition, the buffer factor which specifies the uptake by the surface ocean behaves almost linearly for atmospheric CO_2 concentration as shown in Fig. 9. Only Eq. (5), which describes the uptake by the biosphere, is nonlinear. But it behaves almost linearly when the atmospheric CO_2 concentration is not too high compared with its preindustrial value.

V. SUMMARY

The behavior of the carbon cycle was investigated by using a seven-box model. The model includes the buffer effect for ocean-atmosphere interaction and the logarithmic uptake of CO_2 with a fertilization parameter for the biosphere-

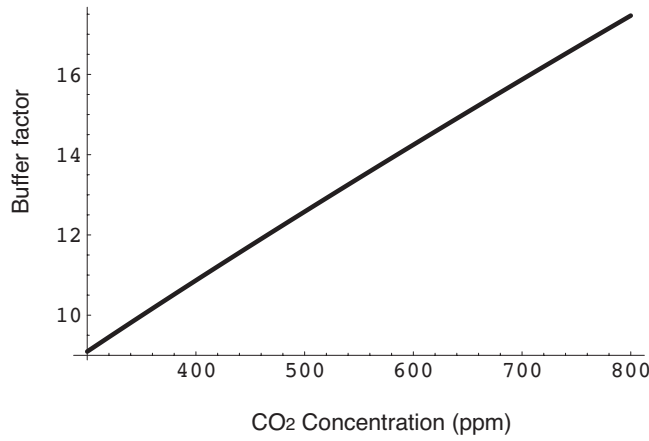


Fig. 9. The buffer factor as a function of atmospheric CO₂ concentration.

atmosphere interaction. The effectiveness of the model was verified by reproducing the trend of atmospheric CO₂ concentration for the past 250 years, the current flux between individual reservoirs, the projection of atmospheric CO₂ concentration based on SRES scenarios, and the derivation of stabilization scenarios for centuries based on WRE profiles. These results imply that the Earth system can be approximated by a linear set of coupled equations.

ACKNOWLEDGMENTS

The author would like to acknowledge the referees for many constructive suggestions.

APPENDIX: THE BUFFER FACTOR

Numerous calculations of the buffer factor exist; we consider Bacastow and Keeling's method here.^{10,23} The buffer factor is defined by the CO₂ concentration P in the atmosphere and the total inorganic carbon concentration C in the surface ocean, under the condition of constant alkalinity A as

$$\xi = \left[\frac{(P - P_0)/P_0}{(C - C_0)/C_0} \right]_{\text{constant alkalinity}}, \quad (\text{A1})$$

where $P_0 = 290.21$ ppm and $C_0 = 2.057 \times 10^{-3}$ mol/l are the preindustrial values of P and C .

The alkalinity A is a measure of the buffering capacity of water and is equal to

$$A = [\text{HCO}_3^-] + 2[\text{CO}_3^{2-}] + [\text{B}(\text{OH})_4^-] + [\text{OH}^-] - [\text{H}^+]. \quad (\text{A2})$$

The brackets denote concentrations; they are related to the following constants;

$$\begin{aligned} K_0 &= \frac{[\text{CO}_2]}{P}, & K_1 &= \frac{[\text{H}^+][\text{HCO}_3^-]}{[\text{CO}_2]}, \\ K_2 &= \frac{[\text{H}^+][\text{CO}_3^{2-}]}{[\text{HCO}_3^-]}, & K_B &= \frac{[\text{H}^+][\text{B}(\text{OH})_4^-]}{[\text{B}(\text{OH})_3]}, \\ K_W &= \frac{[\text{H}^+][\text{OH}^-]}{[\text{H}_2\text{O}]}, \end{aligned} \quad (\text{A3})$$

where by convention $[\text{H}_2\text{O}] = 1$

The total boron and inorganic carbon concentrations are

$$B = [\text{B}(\text{OH})_3] + [\text{B}(\text{OH})_4^-] = \left(1 + \frac{[\text{H}^+]}{K_B} \right) [\text{B}(\text{OH})_4^-], \quad (\text{A4})$$

$$\begin{aligned} C &= [\text{CO}_2] + [\text{HCO}_3^-] + [\text{CO}_3^{2-}] \\ &= PK_0 \left(1 + \frac{K_1}{[\text{H}^+]} + \frac{K_1 K_2}{[\text{H}^+]^2} \right), \end{aligned} \quad (\text{A5})$$

respectively.

With the aid of Eqs. (A3) and (A4), and the substitution x for $[\text{H}^+]$, we write Eq. (A2) as

$$\begin{aligned} x^4 + (A + K_B)x^3 + (AK_B - BK_B - K_W - PK_0K_1)x^2 \\ - (K_BK_W + PK_0K_1(2K_2 + K_B))x - 2PK_0K_1K_B = 0. \end{aligned} \quad (\text{A6})$$

The values of the dissociation constants and alkalinity at the mean ocean temperature 19.6 °C, expressed in moles per liter, are

$$\begin{aligned} K_1 &= 9.747 \times 10^{-7}, & K_2 &= 8.501 \times 10^{-10}, \\ K_B &= 1.881 \times 10^{-9}, & K_W &= 6.463 \times 10^{-15}, \\ B &= 0.409 \times 10^{-3}, & A &= 2.435 \times 10^{-3}, \end{aligned} \quad (\text{A7})$$

and the gas solubility constant at the same temperature is

$$K_0 = 0.03347 \text{ mol/(l atm)} \quad (\text{Ref. 10}). \quad (\text{A8})$$

The buffer factor at an arbitrary atmospheric CO₂ concentration P is calculated as follows. First, x or $[\text{H}^+]$ is solved numerically for the given P from Eq. (A6). Next, the total inorganic carbon concentration C is determined from Eq. (A5) using the solution $[\text{H}^+]$. Finally, the buffer factor is obtained from Eq. (A1) using C and P .

Figure 9 shows the atmospheric CO₂ concentration dependency of the buffer factor. Also, ξ can be approximated as a quadratic function:

$$\xi(z) \approx 3.69 + 1.86 \times 10^{-2}z - 1.80 \times 10^{-6}z^2, \quad (\text{A9})$$

where z is the atmospheric CO₂ concentration of ppm unit.

^aElectronic mail: tommy@nagasaki-u.ac.jp

¹Japan Agency for Marine-Earth Science and Technology, "The Earth Simulator Center," <www.jamstec.go.jp/esc/index.en.html>.

²John Harte, *Consider a Spherical Cow: A Course in Environmental Problem Solving* (University Science Books, Sausalito, CA, 1988).

³H. Oeschger, U. Siegenthaler, U. Schotterer, and A. Gugelmann, "A box diffusion model to study the carbon dioxide exchange in nature," *Tellus* **27**, 168–192 (1975).

⁴R. B. Bacastow and A. Björkström, "Comparison of ocean models for the carbon cycle," in *Carbon Cycle Modelling*, edited by Bert Bolin (Wiley, Chichester, 1981), SCOPE Vol. 16, pp. 29–79.

⁵B. Moore III and B. Bolin, "Oceans, carbon dioxide, and global climate change," *Oceanus* **29** (4), 9–15 (1987).

⁶G. Marland, T. A. Boden, and R. J. Andres, "Global, regional, and national fossil fuel CO₂ emissions," cdiac.ornl.gov/trends/emis/em_cont.htm.

⁷C. D. Keeling, T. P. Whorf, M. Wahlen, and J. van der Plicht, "Interannual extremes in the rate of rise of atmospheric carbon dioxide since 1980," *Nature* (London) **375**(22), 666–670 (1995).

⁸C. D. Keeling and T. P. Whorf, "Atmospheric carbon dioxide record from Mauna Loa," <cdiac.ornl.gov/trends/co2/sio-mlo.htm>.

⁹R. A. Houghton and J. L. Hackler, "Carbon flux to the atmosphere from

- land-use changes," cdiac.ornl.gov/trends/landuse/houghton/houghton.html).
- ¹⁰R. B. Bacastow and C. D. Keeling, "Atmospheric carbon dioxide and radiocarbon in the natural carbon cycle: II. Changes from A. D. 1700 to 2070 as deduced from a geochemical model," in *Carbon and the Biosphere*, edited by G. M. Woodwell and E. V. Pecan (U. S. Atomic Energy Commission, Washington, DC, 1973), pp. 86–135.
 - ¹¹H. S. Kheshgi, A. K. Jain, and D. J. Wuebbles, "Accounting for the missing carbon-sink with the CO₂-fertilization effect," *Clim. Change* **33**, 31–62 (1996).
 - ¹²K. K. Goldewijk, J. G. van Minnen, M. Vloedveld, and R. Leemans, "Simulating the carbon flux between the terrestrial environment and the atmosphere," *Water, Air, Soil Pollut.* **76**, 199–230 (1994).
 - ¹³I. G. Enting, T. M. L. Wigley, and M. Heimann, "Future emission and concentrations of carbon dioxide: Key ocean/atmosphere/land analyses," CSIRO Atmospheric Research, Victoria, Australia, Report No. 31, cmar.csiro.au/e-print/open/enting_2001a1.pdf.
 - ¹⁴W. R. Emanuel, G. G. Killough, W. M. Post, and H. H. Shugart, "Modeling terrestrial ecosystems in the global carbon cycle with shifts in carbon storage capacity by land-use change," *Ecology* **65**(3), 970–983 (1984).
 - ¹⁵M. B. McElroy, "The carbon cycle," in *The Atmospheric Environment: Effects of Human Activity*, edited by M. B. McElroy (Princeton U.P., Princeton, 2002), pp. 141–164.
 - ¹⁶D. M. Etheridge, L. P. Steele, R. L. Langenfelds, R. J. Francey, J.-M. Barnola, and V. I. Morgan, "Historical CO₂ records from the Law Dome DE08, DE08–2, and DSS ice cores," cdiac.ornl.gov/trends/co2/lawdome-data.html).
 - ¹⁷*Climate Change 2001: The Scientific Basis: Contribution of Working Group I to the Third Assessment Report of the Intergovernmental Panel on Climate Change*, edited by J. T. Houghton, Y. Ding, David J. Griggs, M. Noguer, P. J. Van Der Linden, X. Dai, K. Maskell, and C. A. Johnson (Cambridge U.P., Cambridge, 2001).
 - ¹⁸*Climate Change 2007: The Physical Science Basic: Contribution of Working Group I to the Fourth Assessment*, edited by S. Solomon, D. Qin, M. Manning, Z. Chen, M. Marquis, K. B. Averyt, M. Tignor, and H. L. Miller (Cambridge U.P., Cambridge, 2007).
 - ¹⁹T. M. L. Wigley, R. Richels, and J. A. Edmonds, "Economic and environmental choice in stabilization of atmospheric CO₂ concentrations," *Nature (London)* **379**, 240–243 (1996).
 - ²⁰*Special Report on Emissions Scenarios: a Special Report of Working Group III of the Intergovernmental Panel on Climate Change*, edited by Nebojsa Nakicenovic (Cambridge U.P., Cambridge, 2000).
 - ²¹A. K. Jain, H. S. Kheshgi, and D. J. Wuebbles, "Integrated Science model for assessment of climate change," Lawrence Livermore National Laboratory Report No. UCRL-JC-116526, osti.gov/energycitations/product.biblio.jsp?osti_id=10151110.
 - ²²*Emissions Scenarios for the IPCC: An Update, Climate Change 1992: The Supplementary Report to The IPCC Scientific Assessment*, edited by J. Leggett, W. J. Pepper, and R. J. Swart (Cambridge U.P., Cambridge, 1992).
 - ²³C. D. Keeling, "The carbon dioxide cycle: Reservoir models to depict the exchange of atmospheric carbon dioxide with the oceans and land plants," in *Chemistry of the Lower Atmosphere*, edited by S. I. Rasool (Plenum P, New York, 1973).

ALL BACK ISSUES NOW AVAILABLE ONLINE

The contents of the *American Journal of Physics* are available online. AJP subscribers can search and view full text of AJP issues from the first issue published in 1933 to the present. Browsing abstracts and tables of contents of online issues and the searching of titles, abstracts, etc. is unrestricted. For access to the online version of AJP, please visit <http://aapt.org/ajp>.

Institutional and library ("nonmember") subscribers have access via IP addresses to the full text of articles that are online; to activate access, these subscribers should contact AIP, Circulation & Fulfillment Division, 800-344-6902; outside North America 516-576-2270 or subs@aip.org.

Individual ("member") subscribers to the print version who wish (for an additional fee) to add access to the online version should contact AAPT or go to the AAPT website: <https://www.aapt.org/Membership/secure/agreement.cfm>.